Electronic Supplementary Material (ESI) for Journal of Materials Chemistry C.

Electronic supplementary information

for

Multi-stimuli responsive (*L*-tartrato)oxovanadium(V) complex salt with ferroelectric switching and thermistor properties

Marko Dunatov, Andreas Puškarić, and Lidija Androš Dubraja*

Ruđer Bošković Institute, Bijenička cesta 54, 10000 Zagreb, Croatia

Contents

Abbreviations:

1	=	$(TEA)_4[V_4O_8(L\text{-tart})_2]$
1·2H$_2$O	=	$(TEA)_4[V_4O_8(L\text{-tart})_2]\cdot 2H_2O$
1·5H$_2$O	=	$(TEA)_4[V_4O_8(L\text{-tart})_2]\cdot 5H_2O$
1·6H$_2$O	=	$(TEA)_4[V_4O_8(L\text{-tart})_2]\cdot 6H_2O$
1·11H$_2$O	=	$(TEA)_4[V_4O_8(L\text{-tart})_2]\cdot 11H_2O$
$(TEA)^+$	=	$[(C_2H_5)_4N]^+$
(*L*-tart)	=	$(C_4O_6H_2)^{4-}$

Table S1. Crystallographic data and structure refinement details from single-crystal XRD analysis for **1·11H_2O**.

Compound	**1·11H_2O**
Temperature/K	160
Crystal colour, habit	Orange, stick
Empirical formula	$C_{40}H_{106}N_4O_{31}V_4$
M_r/g mol^{-1}	1343.04
Crystal system	orthorhombic
Space group	$P2_12_12_1$
a/Å	13.21820(10)
b/Å	14.01030(10)
c/Å	34.1579(3)
α/°	90
β/°	90
γ/°	90
V/Å^3	6325.73(9)
Z	4
ρ_{calcd}/g cm^{-3}	1.410
μ/mm^{-1}	5.551
F(000)	2856
θ range/°	3.410–79.258
Measured reflections	28959
Independent reflections	12027
Observed reflections	11456
No. of parameters, restraints	817, 33
R_{int}	0.0479
R, wR [$I > 2\sigma(I)$]	0.0355, 0.0908
R, wR [all data]	0.0373, 0.0920
Goodness of fit	1.009
$\Delta\rho_{max}$, $\Delta\rho_{min}$/e Å^{-3}	0.467, -0.412

Table S2. Crystallographic data and structure refinement details from PXRD analysis for **1·11H$_2$O**, **1·6H$_2$O**, **1·5H$_2$O**, **1·2H$_2$O** and **1**.

Compound	**1·11H$_2$O**	**1·6H$_2$O**	**1·5H$_2$O**	**1·2H$_2$O**	**1**
Temperature/K	298	298	313	341	373
Empirical formula	$C_{40}H_{106}N_4O_{31}V_4$	$C_{40}H_{96}N_4O_{26}V_4$	$C_{40}H_{94}N_4O_{30}V_4$	$C_{40}H_{88}N_4O_{27}V_4$	$C_{40}H_{84}N_4O_{25}V_4$
M_r/g mol^{-1}	1343.04	1252.97	1234.95	1180.90	1144.87
Crystal system	Orthorhombic	Monoclinic	Monoclinic	Monoclinic	Monoclinic
Space group	$P2_12_12_1$	$P2_1$	$P2_1$	$C2$	$P2$
a/Å	13.33057(55)	12.29158(77)	12.0512(10)	23.9460(31)	11.7204(22)
b/Å	14.14988(89)	14.0226(13)	13.9832(18)	12.40082(98)	14.0947(31)
c/Å	34.4662(17)	18.3768(12)	18.5996(17)	19.4698(19)	16.7862(31)
α/°	90	90	90	90	90
β/°	90	108.9294(41)	109.4296(48)	103.3871(95)	94.720(14)
γ/°	90	90	90	90	90
V/Å^3	6501.21(58)	2996.12(39)	2955.80(53)	5624.5(10)	2763.59(95)
Z	4	2	2	4	2
Step size/°	0.013	0.013	0.013	0.013	0.013
2θ range/°	4–50	4–50	4–50	5–60	4–50
R_p	0.078	0.0425	0.0384	0.0257	0.0771
R_{wp}	0.0585	0.0542	0.0493	0.0336	0.0979
R_{exp}	0.0423	0.0432	0.0394	0.0333	0.0845
Background	Chebyshev polynomial of 6th order				

Table S3. Hydrogen–bonding geometry in **1·11H$_2$O**.

D–H···*A*	*D*–H/Å	H···*A*/Å	*D*···*A*/Å	*D*–H···*A*/°	Symm. op. on *A*
O(21)–H(21D) ···O(10)	0.87(3)	1.95(3)	2.810(4)	170(4)	*x*, 1 + *y*, *z*
O(21)–H(21E) ···O(20)	0.86(3)	1.94(4)	2.789(4)	171(3)	*x*, *y*, *z*
O(22)–H(22D) ···O(21)	0.85(6)	1.92(5)	2.739(5)	161(7)	*x*, *y*, *z*
O(22)–H(22E) ···O(16)	0.85(3)	1.92(3)	2.768(5)	176(6)	*x*, *y*, *z*
O(23)–H(23D) ···O(31)	0.84(4)	2.11(4)	2.930(4)	167(4)	*x*, 1 + *y*, *z*
O(23)–H(23E) ···O(9)	0.86(4)	2.20(4)	3.011(3)	158(6)	*x*, 1 + *y*, *z*
O(24)–H(24D) ···O(23)	0.86(5)	1.96(5)	2.816(4)	175(6)	*x*, *y*, *z*
O(24)–H(24E) ···O(14)	0.86(4)	1.98(3)	2.823(4)	166(5)	1 + *x*, 1 + *y*, *z*
O(25)–H(25D) ···O(24)	0.86(3)	1.94(3)	2.796(4)	171(6)	*x*, *y*, *z*
O(25)–H(25E) ···O(22)	0.85(3)	1.86(3)	2.716(5)	177(5)	*x*, *y*, *z*
O(26)–H(26D) ···O(27)	0.84(5)	1.93(5)	2.757(4)	169(6)	*x*, *y*, *z*
O(26)–H(26E) ···O(25)	0.87(4)	1.85(4)	2.715(4)	176(6)	*x*, *y*, *z*
O(27)–H(27D) ···O(10)	0.86(5)	2.02(5)	2.865(4)	166(4)	1 + *x*, 1 + *y*, *z*
O(27)–H(27E) ···O(20)	0.85(4)	2.01(5)	2.837(4)	163(6)	1 + *x*, *y*, *z*
O(28)–H(28D) ···O(26)	0.87(3)	1.88(3)	2.746(4)	172(5)	*x*, *y*, *z*
O(28)–H(28E) ···O(19)	0.85(3)	2.02(3)	2.859(4)	170(4)	1 + *x*, *y*, *z*
O(29)–H(29D) ···O(28)	0.87(5)	1.94(5)	2.771(5)	159(4)	*x*, *y*, *z*
O(29)–H(29E) ···O(8)	0.84(5)	2.04(5)	2.793(4)	149(4)	1 + *x*, *y*, *z*
O(30)–H(30D) ···O(29)	0.83(3)	1.97(3)	2.787(4)	170(5)	*x*, *y*, *z*
O(30)–H(30E) ···O(16)	0.84(4)	2.06(4)	2.898(4)	174(4)	*x*, *y*, *z*
O(31)–H(31D) ···O(30)	0.87(4)	2.03(4)	2.879(4)	167(4)	*x*, *y*, *z*
O(31)–H(31E) ···O(7)	0.86(4)	2.03(3)	2.840(3)	156(5)	*x*, *y*, *z*

Table S4. Hydrogen–bonding geometry in $1 \cdot 6H_2O$.

Analysis performed based on crystallographic data in ref. code EDAZOZ.

D–H···*A*	*D*–H/Å	H···*A*/Å	*D*···*A*/Å	*D*–H···*A*/°	Symm. op. on *A*
O(21)–H(85) ···O(25)	0.90	2.02	2.789(7)	143	*x*, *y*, *z*
O(21)–H(86) ···O(2)	0.86	2.13	2.867(6)	144	*x*, *y*, *z*
O(22)–H(87) ···O(18)	1.07	2.28	2.998(6)	122	*x*, *y*, *z*
O(22)–H(88) ···O(4)	1.22	1.75	2.903(6)	156	*x*, *y*, *z*
O(23)–H(89) ···O(5)	1.02	1.90	2.808(7)	147	*x*, 1 + *y*, *z*
O(23)–H(90) ···O(11)	0.93	1.90	2.796(7)	163	*x*, *y*, *z*
O(24)–H(91) ···O(21)	0.97	1.80	2.764(7)	173	1 – *x*, 1/2 + *y*, –*z*
O(24)–H(92) ···O(26)	1.03	1.90	2.810(9)	145	2 – *x*, -1/2 + *y*, –*z*
O(25)–H(93) ···O(5)	1.12	1.75	2.830(6)	162	*x*, *y*, *z*
O(25)–H(94) ···O(11)	1.00	2.00	2.842(6)	141	*x*, –1 + *y*, *z*
O(26)–H(95) ···O(8)	1.01	1.81	2.801(7)	164	*x*, *y*, *z*
O(26)–H(96) ···O(23)	1.13	1.62	2.746(9)	175	*x*, *y*, *z*

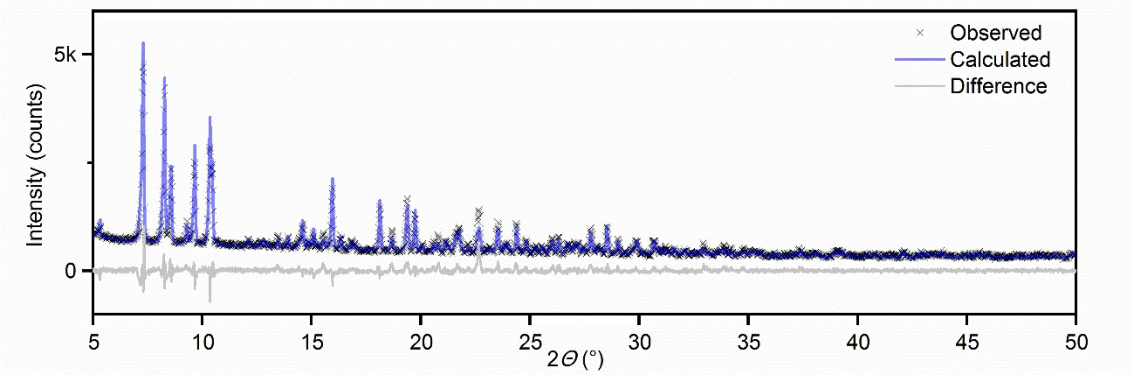

Figure S1. PXRD pattern and profile fitting results for **1·11H_2O** at 298 K.

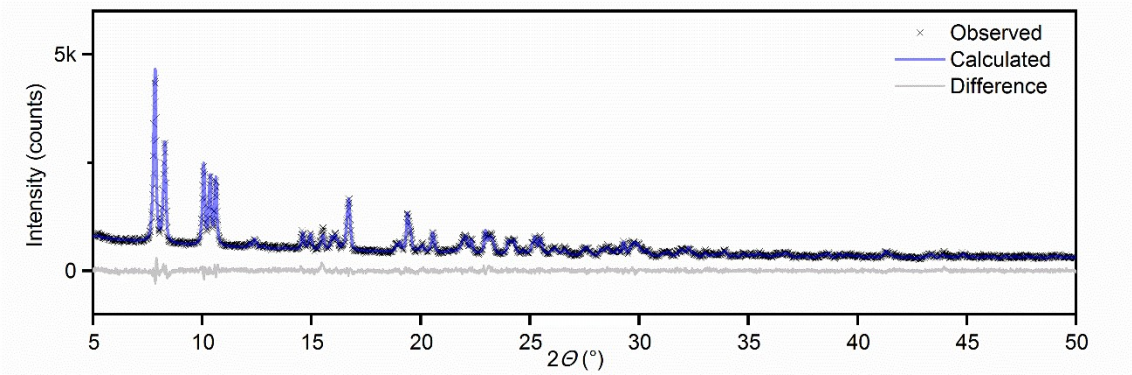

Figure S2. PXRD pattern and profile fitting results for **1·6H_2O** at 298 K.

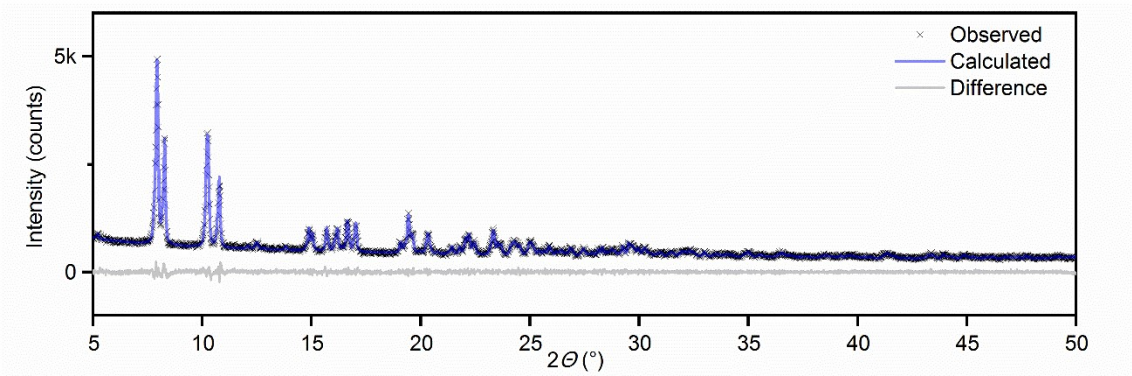

Figure S3. PXRD pattern and profile fitting results for **1·5H_2O** at 313 K.

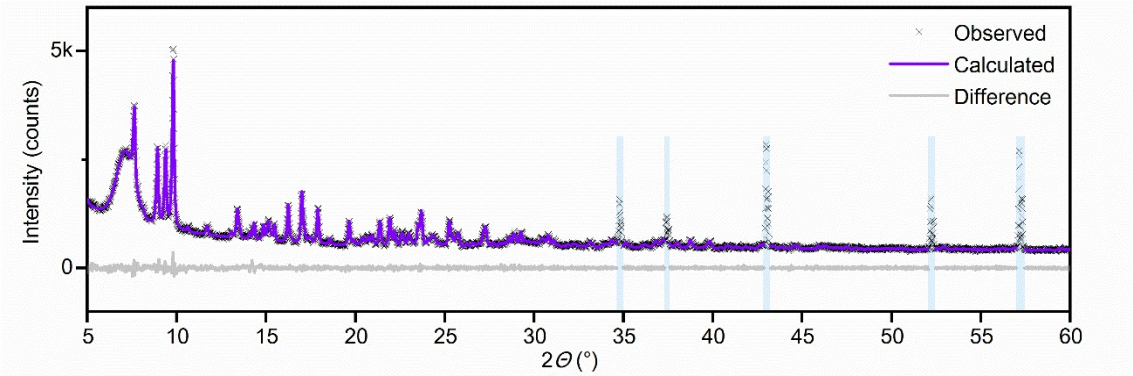

Figure S4. PXRD pattern and profile fitting results for **1·2H$_2$O** at 341 K.

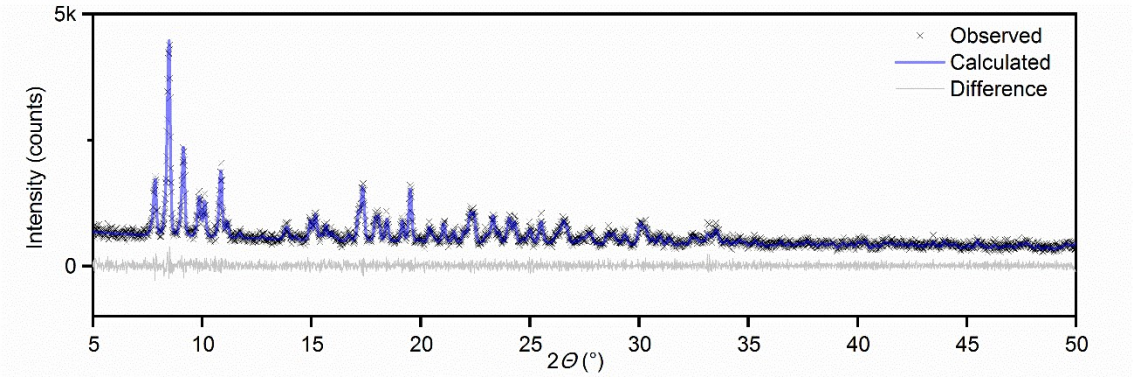

Figure S5. PXRD pattern and profile fitting results for **1** at 373 K.

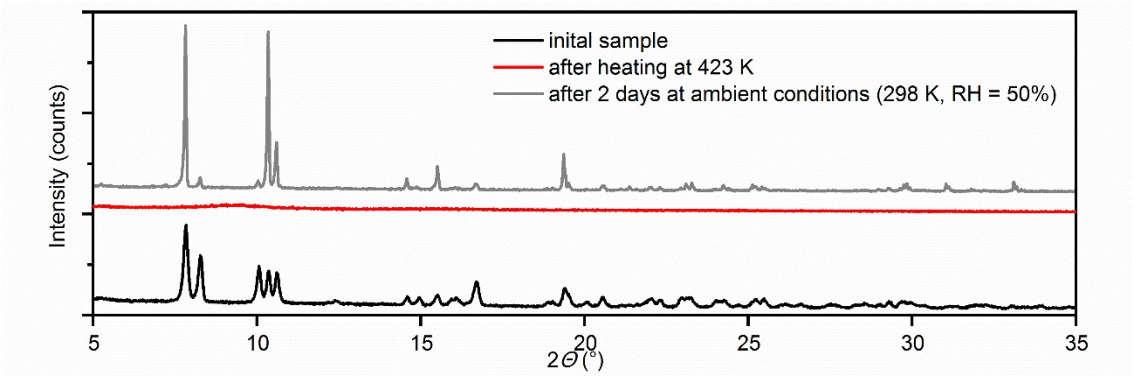

Figure S6. PXRD pattern showing self-recovery process for **1·6H$_2$O**.

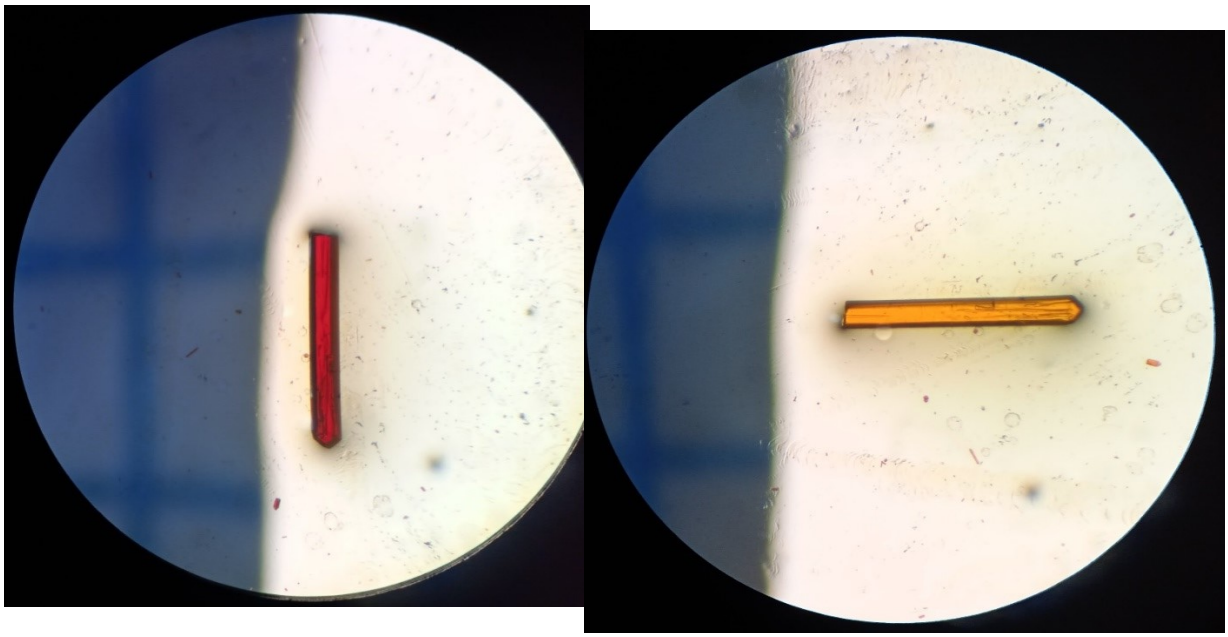

Figure S7. Pleochroism in **1·11H$_2$O**: photograph of a single-crystal changing colour from red to yellow when rotated for 90° under the polarised light.

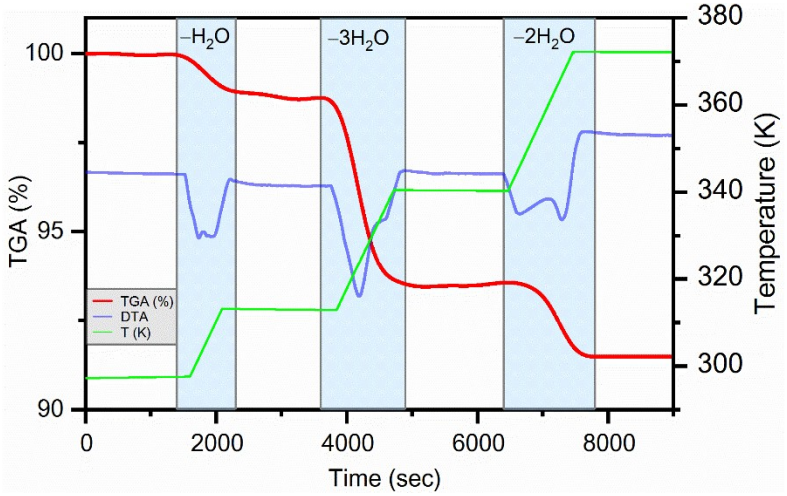

Figure S8. TG/DTA curves for **1·6H$_2$O** measured in isothermal (298 K, 313 K, 341K, 373K) and dynamic conditions (2 K min^{-1}) under a synthetic air atmosphere.

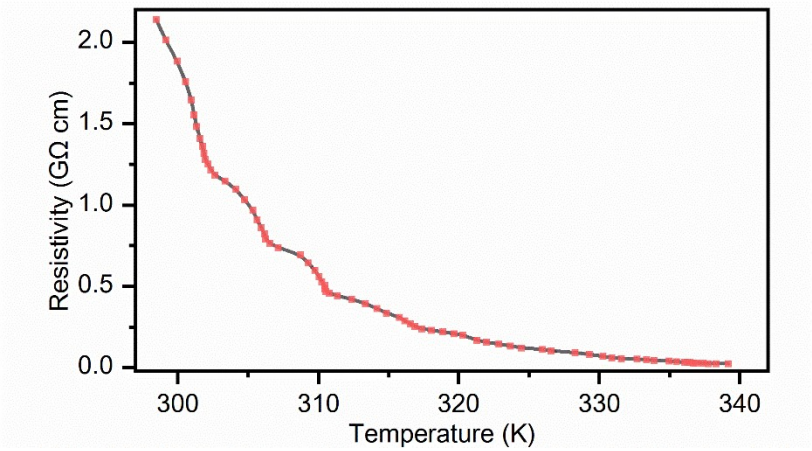

Figure S9. Plot of electrical resistivity versus temperature for **1·5H$_2$O**. The measurement was performed on a pressed pellet attached to silver wires with silver paste contacts. Heating was carried out in an oil bath at a heating rate of 3 K min^{-1}.